RESEARCH ARTICLE

Comparison of two coracoid process transfer techniques on stress shielding using three-dimensional finite-element model

Seyyid Serif Unsal[1], Tugrul Yildirim[2*] and Murat Kayalar[2]

Abstract

Background: We created patient-based 3D finite-element (FE) models that simulate the congruent-arc Latarjet (CAL) and traditional Latarjet (TL) procedures and then compared their stress distribution patterns with different arm positions and glenoid defects.

Methods: The computed tomography data of 10 adult patients (9 men and 1 woman, ages: 18–50 years) were used to develop the 3D FE glenohumeral joint models. Twenty-five and 35% bony defects were created on the anterior glenoid rim, and the coracoid process was transferred flush with the glenoid by the traditional and congruent-arc techniques using two half-threaded screws. A load was applied to the greater tuberosity toward the center of the glenoid, and a tensile force (20 N) was applied to the coracoid tip along the direction of the conjoint tendon. The distribution patterns of the von Mises stress in the traditional and congruent-arc Latarjet techniques were compared.

Results: The mean von Mises on the graft was significantly greater for the TL technique than for the CAL. While the von Mises stress was greater in the distal medial part of the graft in the TL models, a higher stress concentration was observed in the distal lateral edge of the coracoid graft in the CAL models. The proximal medial part of the graft exhibited significantly lower von Mises stress than the distal medial part when compared according to technique, defect size, and arm position. Increasing the glenoid defect from 25 to 35% resulted in a significant increase in stress on the lateral side of the graft in both models.

Conclusion: The stress distribution patterns and stress magnitude of the coracoid grafts differed according to the procedure. Due to placing less stress on the proximal–medial part of the graft, the CAL technique may lead to insufficient stimulation for bone formation at the graft–glenoid interface, resulting in a higher incidence of graft osteolysis.

Clinical relevance The CAL technique may lead to a higher incidence of graft osteolysis.

Level of evidence: Basic Science Study; Computer Modeling.

Keywords: Latarjet procedure, Congruent-arc Latarjet procedure, CT-based finite-element model, Stress shielding, Osteolysis

Introduction

The Latarjet procedure, also known as the coracoid process transfer, is one of the most performed and reliable procedures for treating recurrent anterior shoulder instability in patients with a significant bone defect of the glenoid surface [1–4]. In the traditional Latarjet (TL) procedure, the inferior surface of the coracoid process

*Correspondence: mdtugrul@hotmail.com
[2] Present Address: Private Hand Microsurgery Orthopedics Traumatology (EMOT) Hospital, Kahramanlar District, Street 1418, No:14, Konak, Izmir, Turkey
Full list of author information is available at the end of the article

Unsal *et al. Journal of Orthopaedic Surgery and Research*   (2022) 17:371

Page 2 of 8

(CP) is transferred with the conjoint tendon to the anterior glenoid rim. A "sling effect" is created by the conjoint and subscapularis tendons, and the bony prominence of the transferred coracoid and the ligament effect of the coracoacromial ligaments provide anterior stability [5, 6]. However, the extent to which these effects contribute to stability, at different degrees of abduction and external rotation, is still being debated [7, 8].

Multiple technique modifications to the Latarjet procedure have been reported. For example, Burkhart et al. proposed the "congruent-arc Latarjet" (CAL) technique, in which the coracoid is rotated 90° along its longitudinal axis, allowing the medial surface of the coracoid to be fixed to the anteroinferior of the glenoid and making the inferior surface compatible with the articular surface of the glenoid [3, 9]. Potential advantages of the CAL technique are that it provides a wider surface on which to restore the glenoid defect, it has a slope closer to that of the natural glenoid, and it reduces contact stress around the glenohumeral joint [10–12]. However, multiple biomechanical studies have addressed poor fixation stability as a potential weakness of the CAL technique [13, 14].

Graft osteolysis is a complication of the Latarjet procedure [15, 16]. According to Wolff's law, if loading on a bone increases, the bone will remodel itself over time, and if the loading on a bone decreases, the bone will become weaker. The screws inserted during the Latarjet procedure contribute to the stress shielding in the proximal part of the coracoid graft, which eventually leads to osteolysis in the proximal part [7, 17–19].

A computed tomography (CT)-based 3D finite-element (FE) method has been widely used to assess the stress distribution within the bone to describe the risk of osteolysis [20–23]. By precisely reflecting the bone's architecture, the 3D FE model can visualize the stress distribution inside the bone. Although several studies have investigated the stress distribution in the coracoid graft with a 3D FE model, a comparison of the stress distribution between the CAL and standard TL techniques has not been conducted [18, 19].

In this study, we created patient-based 3D FE models that simulate the CAL and TL procedures, and then compared their stress distribution patterns in different arm positions and glenoid defects. We hypothesized that there would be significant differences in the stress distribution patterns of the two techniques.

Materials and methods
Development of the FE defect model
For the creation of the study's humerus and scapula bone model, the CT data of 10 adult patients (9 males and 1 female, age: 18–50 years) without shoulder trauma were used. The CT data were reconstructed with a slice thickness of 0.1 mm and were transferred to the 3D Slicer software in the DICOM (.dcm) format. The CT data in DICOM format were separated according to appropriate Hounsfield values using 3D Slicer software and converted into a 3D model by segmentation. The model was exported in an .stl format.

Arrangement of the 3D mesh structure and its transformation into a mathematically appropriate solid mesh structure creation of 3D FE analysis models and FE stress analysis were performed on HP workstations equipped with an INTEL Xeon E-2286 processor (2.40 GHz and 64 GB ECC memory). The 3D.stl model of the bone structure created from the CT data was obtained using 3D Slicer software. Reverse engineering and 3D CAD activities were carried out with Altair Evolve software; the Nastran-based Altair Optistruct (Altair, Troy, MI, USA) implicit solver was used to solve the FE models. The mathematical mesh models and the force transfer between the models were created in Altair HyperMesh. The prepared models were placed in the correct 3D space coordinates via the Altair Evolve software, and the modeling process was completed.

The maximum glenoid defect size that could be restored by a TL graft ranged between 19.2% and 38.8% [21]. A maximum defect size of 35% does not exceed the coverage capacity of the TL, while a minimum defect size of 25% necessitates reconstruction of the glenoid bone stock [24, 25] (Fig. 1).

The defect was set parallel to the longitudinal axis of the glenoid according to previous studies [19, 25]. The distal part of the coracoid process (length: 2.5 cm) was resected for simulating the coracoid osteotomy. Cartilage tissue was modeled with reference to the outer surface of the cortical bone, and the trabecular bone was modeled with reference to the inner surface of the cortical bone. On the basis of previous studies, the articular cartilage thickness was determined to be 2.0 mm in both the glenoid and the humeral head [19, 26].

### Simulation of the coracoid transfer
The inferior part of the coracoid was transferred to the anterior glenoid defect to simulate the TL method. To simulate the congruent-arc method, the graft was rotated 90° around the y-axis. Two half-threaded titanium screws (titanium alloy: Ti-6AI-4 V, diameter: 3.5 mm, length: 35 mm) were created similar to commercial models (Depuy Synthes, Raynham, MA, USA) and were used to fix the coracoid process. Care was taken to ensure that the coracoid process was placed flush with the glenoid cartilage. Soft tissues were not modeled in this study.
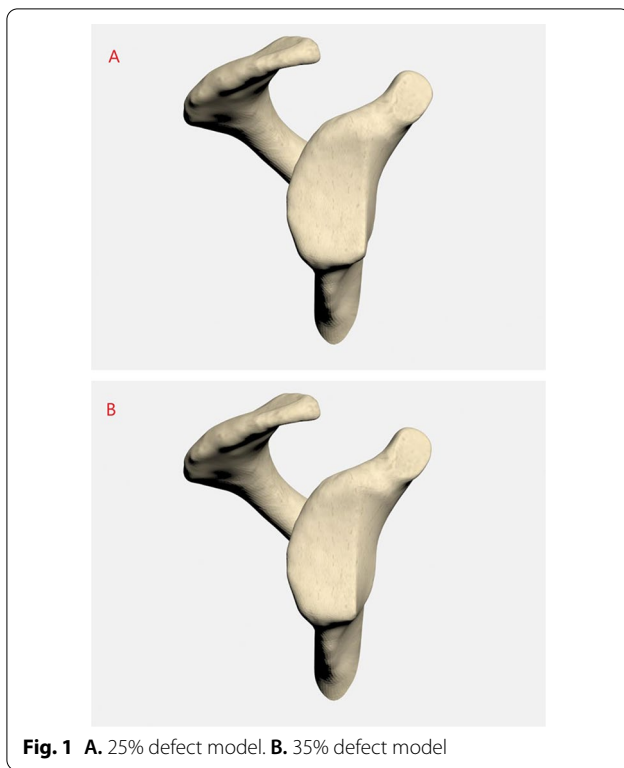
Fig. 1 **A.** 25% defect model. **B.** 35% defect model

Arm position

The initial FE models were created at the hanging arm position in a neutral position. To clarify the stress distribution pattern, a 90° shoulder abduction position was simulated according to previous studies [19, 27] (Fig. 2). The center of the humeral head was determined to be the center of rotation. The abduction angles of the scapula and humerus were 30° and 60°, respectively.
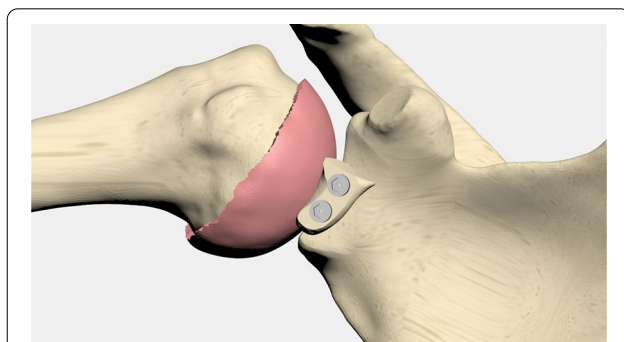
Fig. 2 90^0 abduction position. The center of the humeral head was determined to be the center of rotation. The abduction angles of the scapula and humerus were 30° and 60°, respectively

Contact conditions

In all models, the screw–bone (cortical and trabecular) interface was modeled with friction contact using a coefficient of $\mu = 0.3$; therefore, all models were run nonlinearly, with the exception of the freeze-type contact that was defined in all contact areas (cortical–trabecular, cortical–cortical, and cortical–cartilage) [28]. This approach is based on the assumption that there is no slip at the prestressing interfaces and that the parts move with full correlation during their movement.

Material properties

The linear material properties of the materials were used in the analysis [18, 19]. The elastic modulus and Poisson ratio values of the materials are presented in Table 1.

Boundary conditions

A force of 50 N was applied from the humeral bone head to the glenoid region of the scapula [13, 18, 25]. To simulate the pulling force of the relevant tendon, a force of 20 N was applied from the tip of the coracoid graft to the humerus [18, 19]. The models were fixed by limiting all degrees of freedom from the nodal points located in the distal region of the humeral cortical and trabecular bone and in the medial region of the scapula cortical and trabecular bone.

FE analysis and data interpretation

All models were subjected to elastic analysis by visualizing the distribution pattern of von Mises stress (VMS). Each coracoid graft was divided into four parts (proximal–medial, proximal–lateral, distal–medial, and distal–lateral) to specifically identify the mean VMS of these areas. The stress distribution over the TL and CAL grafts was analyzed for different defect sizes to compare the extent of the stress shielding associated with each procedure.

Statistical analysis

The data analysis was performed with SPSS 26.0, and the data were studied with a 95% confidence level. Because of

Table 1 Material properties

Material	Elastic modulus (MPa)	Poisson ratio
Humerus cortical bone	13,400	0.3
Humerus trabecular bone	2000	0.3
Scapula cortical bone	10,000	0.3
Scapula trabecular bone	1000	0.4
Titanium screw	113,800	0.3
Biceps tendon	35	0.49

Unsal *et al. Journal of Orthopaedic Surgery and Research*   (2022) 17:371

Page 4 of 8

the small sample size, nonparametric methods were used in the study, as well as Mann–Whitney and Kruskal–Wallis tests.

Results

The mean VMS values for all scenarios are summarized in Fig. 3.

The mean VMS on the graft was significantly greater in the TL technique than in the CAL technique in the 25 and 35% defect models ($p > 0.05$). The stress distribution patterns of the coracoids differed according to the procedure: while the VM stress was greater in the distal medial part of the graft in the TL models, a higher stress concentration was observed in the distal lateral edge of the coracoid graft in the CAL models ($p > 0.05$) (Fig. 4). In all models, the proximal part of the grafts exhibited significantly less VMS ($p > 0.05$).

Increasing the glenoid defect from 25 to 35% resulted in a significant increase in stress on the lateral side of the graft in both models ($p > 0.05$). However, there was no significant increase or decrease in the VMS in the remaining parts of the graft for either technique. In the 90° abduction models, significantly greater VMS was observed in both the CAL and TL grafts than in the neutral position models ($p > 0.05$).

Discussion

To our knowledge, this is the first study comparing stress distribution patterns between the TL and the CAL procedures. Since the Latarjet procedure is a non-anatomical augmentation of the glenoid surface, it can alter the intra-articular stress distribution dramatically. Previous biomechanical and FE model studies have shown that graft osteolysis is expected in the proximal part of the graft in the LT technique [18, 19]. However, no studies have been performed to describe the stress distribution and its magnitude in the CAL procedure. This study clearly demonstrated, as we expected, that the stress distribution patterns and stress magnitude of the coracoid grafts differ according to the procedure. These differences may be attributed to the increased surface contact with the humeral head in the CAL model, which may have resulted in less mean stress on the graft and relatively greater stress concentration on the lateral edge. Alternatively, with the TL model, higher stress was observed in the medial part of the graft where bony consolidation was expected. The lack of mechanical stimuli in certain areas of the coracoid graft can contribute to osteolysis in these areas. [7, 29]

That the medial stress is less in the CAL technique than in the TL may cause insufficient stimulation for bone formation at the graft–glenoid interface, which could eventually lead to a greater incidence of graft osteolysis
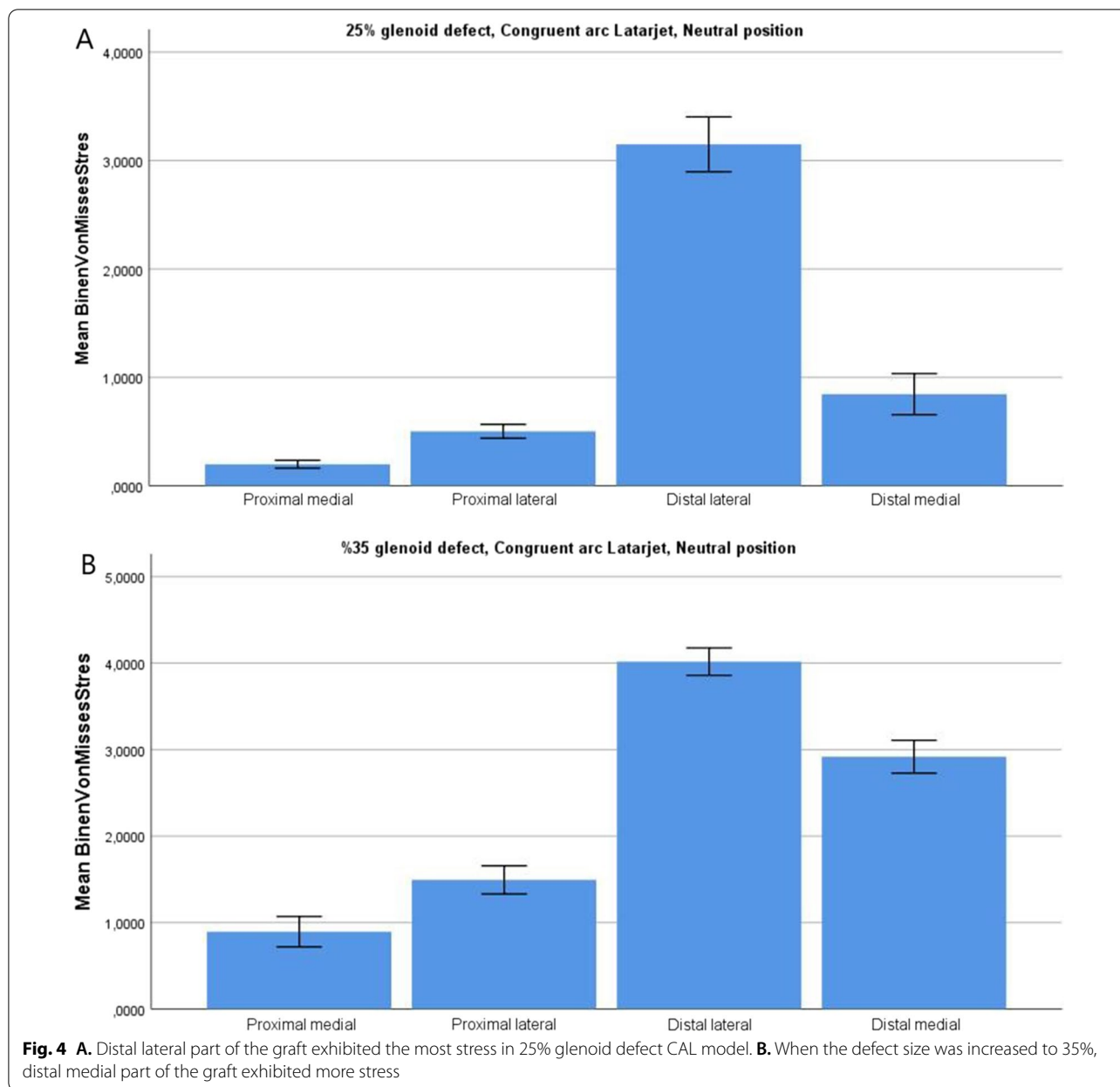
or nonunion. Mengers et al. analyzed 26 studies comparing TL and CAL techniques, identifying that the fibrous or nonunion incidence was greater for the CAL technique [30]. Graft osteolysis may occur if a larger than necessary graft is used because the graft does not experience adequate forces from the humeral head and subsequently resorbs in accordance with Wolff's law [17]. Some authors have proposed that when a smaller defect is filled using the CAL technique, the width of the graft size should be reduced to prevent stress shielding [14]. We observed a significant increase in stress on the CAL graft when the glenoid defect was increased from 25 to 35%. Previous studies have reported that up to 53% of the glenoid may be restored using the CAL technique. Considering our findings and previous studies, the CAL technique should not be used for small defects.

Less stress was observed at the proximal half of the coracoid bone graft in both the TL and CAL techniques for both glenoid defects and arm positions. A high stress concentration was identified at the distal part of the coracoid graft caused by the tensile force created by the conjoint tendon. Similar to the findings of Sano et al., the proximal–medial part represented the lowest equivalent stress of the four parts of the coracoid graft in both models [18, 19]. The insertion of two screws may have shielded the proximal half of the coracoid from the tensile force of the conjoint tendon. These findings indicate that the proximal–medial part of the graft may have the highest risk of osteolysis, regardless of the technique.

Latarjet is one of the most widely used surgical procedures for treating significant bone defects of the glenoid surface and failed Bankart repairs [2–4]. Although the TL procedure is effective for the management of recurrent anterior shoulder instability, it is not without complications. Coracoid graft osteolysis and fibrous nonunions are considered the main causes of recurrent dislocation, pain, and stiffness in patients after the Latarjet procedure [7, 31]. Hurley et al. evaluated 13 studies with a minimum follow-up of 10 years in patients who underwent the TL procedure and found 8.5% dislocation recurrence and 3.7% revision rates [16]. To replace the articular shape of the glenoid, Burkhart et al. proposed the "congruent-arc" technique, in which the graft is rotated 90° along its longitudinal axis, thus allowing the medial surface of the coracoid to fix to the anteroinferior of the glenoid and making the inferior surface compatible with the articular surface of the glenoid [3]. Because the radius of the curvature of the inferior face of the coracoid graft is similar to that of the native glenoid, it is possible to reconstruct larger glenoid defects, providing a more significant bone-blocking effect and decreasing the contact pressure across the glenohumeral joint [10, 13, 32, 33]. In a recent meta-analysis comparing the TL and CAL modifications,
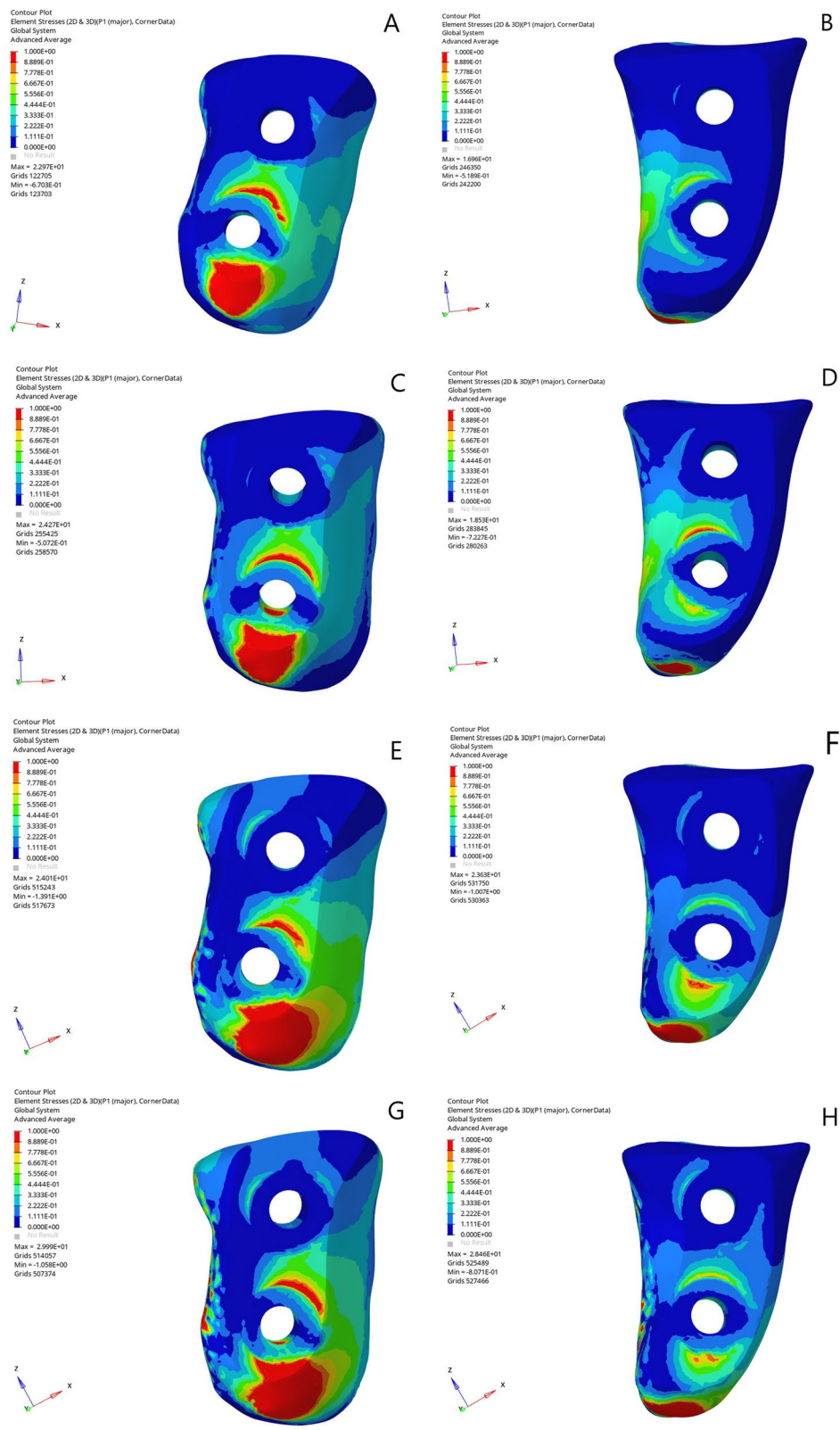
Fig. 3 **A.** TL, 25% glenoid defect, neutral arm position. **B.** CAL, 35% glenoid defect, neutral arm position. **C.** TL, 35% glenoid defect, neutral arm position. **D.** CAL, 35% glenoid defect, neutral arm position. **E**. TL, 25% glenoid defect, 90^0 abduction position. **F.** CAL, 25% glenoid defect, 90^0 abduction position. **G.** TL, 35% glenoid defect, 90^0 abduction position. **H.** CAL, 35% glenoid defect, 90^0 abduction position

Unsal *et al. Journal of Orthopaedic Surgery and Research* (2022) 17:371

Page 6 of 8

Fig. 4 A. Distal lateral part of the graft exhibited the most stress in 25% glenoid defect CAL model. **B.** When the defect size was increased to 35%, distal medial part of the graft exhibited more stress

patients undergoing CAL were less likely to have recurrent subluxation, postoperative complications, and reoperations and were more likely to return to sports and activities. [30]

The small contact area between the graft and glenoid makes the CAL technique significantly less resistant to load to failure compared with the TL tchnique [13, 14]. In addition, there is a shorter bone distance around the screw with the CAL technique, which makes it very difficult to perform in patients with small coracoids [34]. Moreover, a higher incidence of broken, loose, or improperly placed screws have been reported with the

CAL technique, although no difference was observed in graft positioning [30]. Male patients were significantly more likely to undergo augmentation using the CAL technique. When deciding on which technique to use, the patient's coracoid width and size of the glenoid defect should be considered.

This study has the following limitations. First, we did not perform the analysis on a 3D dynamic motion model of the shoulder joint. Future studies, including dynamic analyses, are necessary to describe the true biomechanical environment created following the TL and CAL techniques. Second, there were numerous

Unsal *et al. Journal of Orthopaedic Surgery and Research*   (2022) 17:371

Page 7 of 8

assumptions with respect to the material properties, as well as the boundary and contact conditions, each of which may have affected the results. Third, our results were not subjected to further biomechanical validation because of the technical difficulties associated with measuring the actual stress distribution during cadaveric testing. However, because our results are consistent with those of previous studies, we believe our simulation is an effective and accurate recreation of real-world conditions.

Conclusion

The TL and CAL techniques exhibited different stress distribution patterns and stress magnitudes on coracoid grafts. Although the CAL modification provides a more significant bone-blocking effect and decreases the contact pressure across the glenohumeral joint, less stress on the medial part of the graft may lead to insufficient stimulation for bone formation at the graft–glenoid interface, which could eventually lead to a higher incidence of graft osteolysis. Surgeons should be aware of this risk when considering the CAL technique, especially for small glenoid defects not exceeding 35% of glenoid width.

Abbreviations
FE: Finite element; TL: Traditional Latarjet; CAL: Congruent-arc Latarjet; VMS: Von Mises stress; CT: Computed tomography; CP: Coracoid process.

Declarations

Ethics approval and consent to participate
The study was carried out following ethical standards under the Declaration of Helsinki of 1964. The acquisition of CT images was approved by the Ethics Committee of the SBU Kanuni Research and Education Hospital, Trabzon, Turkey (approval no: 2022/19), and written consent was obtained from the volunteers.

Consent for publication
The patients enrolled in the study agreed to the use of the data for research and to authorize its publication.

Competing interests
The authors declare that they have no competing interests.

Author details
¹Trabzon Kanuni Research and Education Hospital, Trabzon, Turkey. ²Present Address: Private Hand Microsurgery Orthopedics Traumatology (EMOT) Hospital, Kahramanlar District, Street 1418, No:14, Konak, Izmir, Turkey.

References
1. Latarjet M. Technic of coracoid preglenoid arthroereisis in the treatment of recurrent dislocation of the shoulder. Lyon Chir. 1958;54(4):604–7.
2. Joshi MA, Young AA, Balestro JC, Walch G. The Latarjet-Patte procedure for recurrent anterior shoulder instability in contact athletes. Orthop Clin North Am. 2015;46(1):105–11.
3. Burkhart SS, De Beer JF, Barth JR, Cresswell T, Roberts C, Richards DP. Results of modified Latarjet reconstruction in patients with anteroinferior instability and significant bone loss. Arthroscopy. 2007;23(10):1033–41.
4. Rossi LA, Tanoira I, De Cicco FL, Ranalletta M. Traditional versus congruent-arc Latarjet anatomic and biomechanical perspective. EFORT Open Rev. 2021;6(4):280–7.
5. Dines JS, Dodson CC, McGarry MH, Oh JH, Altchek DW, Lee TQ. Contribution of osseous and muscular stabilizing effects with the Latarjet procedure for anterior instability without glenoid bone loss. J Shoulder Elbow Surg. 2013;22(12):1689–94.
6. Mizuno N, Denard PJ, Raiss P, Melis B, Walch G. Long-term results of the Latarjet procedure for anterior instability of the shoulder. J Shoulder Elbow Surg. 2014;23(11):1691–9.
7. Di Giacomo G, Costantini A, de Gasperis N, De Vita A, Lin BK, Francone M, et al. Coracoid graft osteolysis after the Latarjet procedure for anteroinferior shoulder instability: a computed tomography scan study of twenty-six patients. J Shoulder Elbow Surg. 2011;20(6):989–95.
8. Yamamoto N, Muraki T, Sperling JW, Steinmann SP, Cofield RH, Itoi E, et al. Stabilizing mechanism in bone-grafting of a large glenoid defect. J Bone Joint Surg Am. 2010;92(11):2059–66.
9. de Beer JF, Roberts C. Glenoid bone defects–open latarjet with congruent arc modification. Orthop Clin North Am. 2010;41(3):407–15.
10. Armitage MS, Elkinson I, Giles JW, Athwal GS. An anatomic, computed tomographic assessment of the coracoid process with special reference to the congruent-arc latarjet procedure. Arthroscopy. 2011;27(11):1485–9.
11. Dehaan A, Munch J, Durkan M, Yoo J, Crawford D. Reconstruction of a bony bankart lesion: best fit based on radius of curvature. Am J Sports Med. 2013;41(5):1140–5.
12. Noonan B, Hollister SJ, Sekiya JK, Bedi A. Comparison of reconstructive procedures for glenoid bone loss associated with recurrent anterior shoulder instability. J Shoulder Elbow Surg. 2014;23(8):1113–9.
13. Giles JW, Puskas G, Welsh M, Johnson JA, Athwal GS. Do the traditional and modified latarjet techniques produce equivalent reconstruction stability and strength? Am J Sports Med. 2012;40(12):2801–7.
14. Montgomery SR, Katthagen JC, Mikula JD, Marchetti DC, Tahal DS, Dornan GJ, et al. Anatomic and biomechanical comparison of the classic and congruent-arc techniques of the Latarjet procedure. Am J Sports Med. 2017;45(6):1252–60.
15. Chillemi C, Guerrisi M, Paglialunga C, Salate Santone F, Osimani M. Latarjet procedure for anterior shoulder instability: a 24-year follow-up study. Arch Orthop Trauma Surg. 2021;141(2):189–96.
16. Hurley ET, Jamal MS, Ali ZS, Montgomery C, Pauzenberger L, Mullett H. Long-term outcomes of the Latarjet procedure for anterior shoulder instability: a systematic review of studies at 10-year follow-up. J Shoulder Elbow Surg. 2019;28(2):e33–9.
17. Giacomo GD, Costantini A, de Gasperis N, De Vita A, Lin BK, Francone M, et al. Coracoid bone graft osteolysis after Latarjet procedure: a comparison study between two screws standard technique vs mini-plate fixation. Int J Shoulder Surg. 2013;7(1):1–6.
18. Sano H, Komatsuda T, Abe H, Ozawa H, Kumagai J, Yokobori TA Jr. Intra-articular biomechanical environment following modified Bristow and Latarjet procedures in shoulders with large glenoid defects: Relationship with postoperative complications. J Shoulder Elbow Surg. 2021;30(10):2260–9.

Unsal *et al. Journal of Orthopaedic Surgery and Research*   (2022) 17:371

Page 8 of 8

19. Sano H, Komatsuda T, Abe H, Ozawa H, Yokobori TA Jr. Proximal-medial part in the coracoid graft demonstrates the most evident stress shielding following the Latarjet procedure: a simulation study using the 3-dimensional finite element method. J Shoulder Elbow Surg. 2020;29(12):2632–9.
20. Thompson SM, Yohuno D, Bradley WN, Crocombe AD. Finite element analysis: a comparison of an all-polyethylene tibial implant and its metal-backed equivalent. Knee Surg Sports Traumatol Arthrosc. 2016;24(8):2560–6.
21. Inal S, Gok K, Gok A, Pinar AM, Inal C. Comparison of biomechanical effects of different configurations of Kirschner wires on the epiphyseal plate and stability in a Salter-Harris type 2 distal femoral fracture model. J Am Podiatr Med Assoc. 2019;109(1):13–21.
22. Inal S, Taspinar F, Gulbandilar E, Gok K. Comparison of the biomechanical effects of pertrochanteric fixator and dynamic hip screw on an intertrochanteric femoral fracture using the finite element method. Int J Med Robot. 2015;11(1):95–103.
23. Gregori M, Eichelberger L, Gahleitner C, Hajdu S, Pretterklieber M. relationship between the thickness of the coracoid process and Latarjet graft positioning-an anatomical study on 70 embalmed scapulae. J Clin Med. 2020. https://doi.org/10.3390/jcm9010207.
24. Beran MC, Donaldson CT, Bishop JY. Treatment of chronic glenoid defects in the setting of recurrent anterior shoulder instability: a systematic review. J Shoulder Elbow Surg. 2010;19(5):769–80.
25. Yamamoto N, Muraki T, An KN, Sperling JW, Cofield RH, Itoi E, et al. The stabilizing mechanism of the Latarjet procedure: a cadaveric study. J Bone Joint Surg Am. 2013;95(15):1390–7.
26. Schleich C, Bittersohl B, Antoch G, Krauspe R, Zilkens C, Kircher J. Thickness distribution of glenohumeral joint cartilage. Cartilage. 2017;8(2):105–11.
27. Boons HW, Giles JW, Elkinson I, Johnson JA, Athwal GS. Classic versus congruent coracoid positioning during the Latarjet procedure: an in vitro biomechanical comparison. Arthroscopy. 2013;29(2):309–16.
28. Chen F, Huang X, Ya Y, Ma F, Qian Z, Shi J, et al. Finite element analysis of intramedullary nailing and double locking plate for treating extra-articular proximal tibial fractures. J Orthop Surg Res. 2018;13(1):12.
29. Haeni DL, Opsomer G, Sood A, Munji J, Sanchez M, Villain B, et al. Three-dimensional volume measurement of coracoid graft osteolysis after arthroscopic Latarjet procedure. J Shoulder Elbow Surg. 2017;26(3):484–9.
30. Mengers SRP, Knapik DM, Kaufman MW, Edwards G, Voos JE, Gillespie RJ, et al. Clinical outcomes of the traditional latarjet versus the congruent arc modification for the treatment of recurrent anterior shoulder instability: a meta-analysis. Orthop J Sports Med. 2021;9(10):23259671211030204. https://doi.org/10.1177/23259671211030204.
31. Di Giacomo G, de Gasperis N, Costantini A, De Vita A, Beccaglia MA, Pouliart N. Does the presence of glenoid bone loss influence coracoid bone graft osteolysis after the Latarjet procedure? A computed tomography scan study in 2 groups of patients with and without glenoid bone loss. J Shoulder Elbow Surg. 2014;23(4):514–8.
32. Bhatia DN, Kandhari V. Bone defect-induced alteration in glenoid articular surface geometry and restoration with coracoid transfer procedures: a cadaveric study. J Shoulder Elbow Surg. 2019;28(12):2418–26.
33. Ghodadra N, Gupta A, Romeo AA, Bach BR Jr, Verma N, Shewman E, et al. Normalization of glenohumeral articular contact pressures after Latarjet or iliac crest bone-grafting. J Bone Joint Surg Am. 2010;92(6):1478–89.
34. Dumont GD, Vopat BG, Parada S, Cohn R, Makani A, Sanchez G, et al. Traditional versus congruent arc Latarjet technique: effect on surface area for union and bone width surrounding screws. Arthroscopy. 2017;33(5):946–52.

Publisher's Note